P1.101 MINERAL DUST TRANSPORT OVER WEST AFRICA IN 2006

Juliane Schwendike[1] * Diana Bou Karam[2], Suzanne Crumeyrolle[3,4], Cyrille Flamant[2], Sarah Jones[1], Manuel Schmidberger[1], Fabien Solmon[5], Tanja Stanelle[1,6], Pierre Tulet[4], Heike Vogel[1], and Bernhard Vogel[1]

1 Karlsruher Institut für Technologie, Karlsruhe, Germany
2 LATMOS/IPSL, CNRS, Universite Pierre et Marie Curie, Paris, France
3 GAME/CNRM, METEO-FRANCE - CNRS, Toulouse, France
4 LaMP, 24 rue des Landais, 63177 Aubiere Cedex,France
5 Laboratoire d'Aerologie, Toulouse, France
6 now at ETH Zurich, Switzerland

1. INTRODUCTION

North Africa is the largest source of mineral dust, and the dust plumes emanating from this region are the most wide spread, persistent and dense. The dust is emitted from the desert regions and transported into the atmosphere. These processes are highly variable in time and space with an annual peak during summer. The uplifted dry and mineral dust particle enriched air, the so called Saharan air layer (SAL), is transported over West Africa and over the Atlantic, where it can affect the cyclogenesis of tropical cyclones. Dust emission over North Africa can occur in association with a variety of different weather systems.

- High near–surface wind speeds result from the downward mixing of momentum from nocturnal low–level jets. These can occur in relation to Saharan heat low dynamics (Knippertz, 2008) or with low–level jets generated in the lee of complex terrain, e.g. the Bodélé region in Northern Chad (Washington and Todd, 2006; Todd et al., 2008).
- The penetration of upper level troughs to low latitudes (Knippertz and Fink, 2006).
- Density currents due to strong evaporational cooling along precipitating cloud bands over the northern Sahara (Knippertz and Fink, 2006) and along the Saharan side of the Atlas Mountain chain in southern Morocco (Knippertz et al., 2007).
- The density currents due to mesoscale convective systems (MCSs) are very effective for the emission of dust and its injection to altitudes favourable for long–range transport. This process is of particular importance at the beginning of the monsoon season, before the growing vegetation rapidly inhibits local dust emission (Flamant et al., 2007).
- Highly turbulent winds at the leading edge of the monsoon nocturnal flow in the Inter Tropical Discontinuity (ITD) region also generate dust uplifting (Bou Karam et al., 2008). The thermodynamic characteristics of the dusty layer at the leading edge of the monsoon flow over the Sahel are described by Marsham et al. (2008).
- Density currents at the leading edge of the Atlantic inflow (Grams et al., 2010) in association with dust uplift were observed in model simulations by Schwendike (2010).

We compare the monthly mean dust concentrations based on a regional climate model for the months of 2006. Additionally, selected dust events are simulated with non-hydrostatic mesoscale models. The mass flux along fixed cross sections from these runs is compared with the results from the regional climate model. The case studies chosen are an intense dust event between about 5-11 March 2006 associated with a cold surge of extra–tropical origin, a pre–summer monsoon event (8-14 June 2006), a summer monsoon event (2-10 July 2006), and a smaller dust event during the late summer monsoon (9-14 September 2009). The transport of mineral dust for these events will be investigated in the following.

2. NUMERICAL MODELS

This study is based on the model output from the third generation regional climate modelling system RegCM (Giorgi et al., 1993; Pal et al., 2007) and two mesoscale models Meso-NH (Lafore et al., 1998) and COSMO-ART (Doms and Schättler, 2002; Vogel et al., 2009).

In RegCM, the emission, transport and deposition of mineral dust particles is computed by an online coupled dust scheme (Zakey et al., 2006). Prognostic mineral dust bin concentrations are used to calculate the longwave emissivity and absorptivity. The longwave absorption cross sections and the refractive indices are consistent with Wang et al. (2006). Standard dust optical properties are used (Solmon et al., 2008). The model runs used in the present study have a horizontal resolution of 60 km. Regional simulations for the period 1996–2006 are conducted by Solmon et al. (2008).

The dust aerosols are parametrised in Meso-NH (Grini et al., 2006). The dust emission scheme is the

* *Corresponding author address:* Juliane Schwendike, Karlsruher Institut für Technologie, Kaiserstr. 12, 76131 Karlsruhe, Germany; e-mail: juliane.schwendike@kit.edu

Dust Entrainment And Deposition (DEAD) model (Zender et al., 2003), that calculates dust fluxes from wind friction velocity and is implemented as a component of Meso-NH (Grini et al., 2006). Entrainment thresholds for saltation, moisture inhibition and saltation feedback are included in DEAD. Transport and loss processes are computed by the ORILAM model (Tulet et al., 2005) by following the evolution of two moments of three lognormal modes defined by Alfaro and Gomes (2001). Dust advection and diffusion are quantified by the transport processes and methods used in Meso-NH. This includes the advection by the resolved wind field, shallow convective transport, and mixing within the planetary boundary layer (PBL). The short- and longwave radiative fluxes are computed using the same radiative scheme as the ECMWF model. The shortwave radiative fluxes are computed for six wavelengths using the extinction coefficients, asymmetry factors and single scattering albedo provided by lookup tables.

COSMO-ART (COSMO: Consortium for Small–scale Modelling, ART: Aerosols and Reactive Trace gases) is a recently developed model system which describes the emission, the transport and the deposition of gases and aerosols and their feedback with the state of the atmosphere (Vogel et al., 2009). The model system is fully coupled online and identical numerical methods are applied to calculate the transport of all scalars. The interaction of the mineral dust particles with cloud microphysics is neglected. Mineral dust particles are represented by log normal distributions. Emission of dust particles are calculated online as functions of friction velocity, soil moisture and surface parameters (Alfaro and Gomes, 2001; Vogel et al., 2006; Stanelle et al., 2010).

Both mesoscale models used ECMWF operational analyses as initial and boundary data, whereas RegCM used NCEP2 reanalysis data. Details on the model runs used in this study can be found in Tab. 1.

3. MINERAL DUST EVENTS DURING 2006 AND THE RELATED DUST TRANSPORT ACROSS WEST AFRICA

The distribution of mineral dust over West Africa in 2006, based on the RegCM model runs, shows a large temporal and spatial variability. The highest aerosol optical thicknesses (AOTs) occur throughout the year in Mauritania and Niger (Fig. 1). The amount of mineral dust in the atmosphere over West Africa is smallest in January. The AOT is markedly increased in March due to an intense dust event associated with a cold front that crossed the Atlas Mountains and moved across West Africa (section 3.1). In April and May, high AOTs occur in a zonal band between 12 °N and 22 °N with their centre over Niger and at the coast of Mauritania and Senegal. The largest amount of dust in the atmosphere can be observed between June and August, in accordance with Engelstaedter and Washington (2007). Large parts of the Sahara and the Sahel show high AOTs. During this period large amounts of dust are advected westward from the Bodélé depression (Washington and Todd, 2006; Todd et al., 2008). Several dust outbreaks occur due to the gust fronts of MCSs (section 3.2), orographically canalisation effects of, for instance, the Harmattan winds (section 3.2, 3.3), and at the ITD (section 3.3). Especially between June and September, large amounts of dust are transported over the Atlantic. This transport can be related to African Easterly jet (AEJ) (e.g. section 3.4). The highest AOTs over the eastern Atlantic occurred in August (Fig. 1h). The atmospheric dustload is markedly reduced in September, and decreases further during the remaining months of 2006. However, relatively large AOTs occur in Niger in November.

The cross sections of aerosol mass flux and mass concentrations averaged over the months May to September (Fig. 2) show that the largest dust concentrations occur along 10 °W (Fig. 2g) between 17-24 °N, and below 700 hPa over the western Sahara. The dust is transported westward by the AEJ with its maximum at about 600 hPa, and eastwards by the monsoon flow south of 20 °N (Fig. 2c). Along 15 °W, the dust source region has a larger horizontal extend (16-25 °N) and the highest mass concentrations are restricted to the lowest 200 hPa (Fig. 2b,f). The penetration of the monsoon flow reaches further north than in any other of the four cross sections. Two dust concentration maxima (Fig. 2d,h) occur along 10 °E. One is located between 15-19 °N and extends up to about 700 hPa and the other between 25-28 °N extending up to about 800 hPa. Large parts of the southern dust maximum occur in the monsoon layer and are transported eastwards. Above, the AEJ is responsible for the fast transport westwards (Fig. 2b). Weaker dust concentrations can be found up to about 500 hPa and even higher altitudes in the other cross sections. The smallest dust concentrations and thus, mass fluxes occurs along 20 °W due to dry and wet deposition of the aerosol particles.

3.1 *COLD AIR OUTBREAK IN MARCH*

On 5 March 2006, a cold front moved from Spain towards the south over Morocco and Algeria and a high pressure system occurred over the Atlantic. Both systems moved further to the east on 6 March 2006. The cold front crossed the Atlas Mountains in Morocco and northern Algeria leading to an uplift of mineral dust in the lee of the mountains, marking the beginning of a major dust storm in West Africa. The dust storm moved together with the cold front towards the southwest, south and southeast. The peak intensity of the dust storm occurred on 7 March 2006 due to orographical induced high emission rates at the Hoggar, Aïr and Tibesti Mountains.

This significant dust event was simulated with COSMO-ART (initialised on 5 March 2006, 00 UTC) and is compared to a RegCM (initialised on 15 February 2006, 00 UTC) run. It is apparent that both models represent the position of the event nicely. The AOT is generally higher in the COMSO-ART run and the event appears to be simulated quite realistically. The lower AOT values in the RegCM run can be explained partially by the fact that

the northern model boundary was located at 30 °N. The cold front led to significant dust uplift north of this latitude, which is not taken into account in the RegCM simulation but contributes to the dust concentrations in the COSMO-ART run. A detailed description of this case study and the comparison with observations can be found in Stanelle (2008); Stanelle et al. (2010).

The mass flux of the dust concentration along 15 °W, 10 °W, 10 °E (Fig. 3) show high mass fluxes north of 22 °N. At 15 °W the dust is concentrated below 800 hPa and transported eastward by the front. South of 14 °N, the dust is lifted up and reaches a wind maximum at the height of about 750 hPa and 9 °N (Fig. 3f). A similar situation occurs along 10 °W, but the mass flux is higher and extends up to about 700 hPa. The top of the dust layer in this region is slightly lower in the RegCM simulation. In the RegCM run, the dust is lifted up south of 14 °N and south of 12 °N in the COSMO-ART run. Along 10 °E, aerosol mass flux is predominately directed towards the east. It reaches heights up to 550 hPa north of 16 °N. Over the Atlantic, the mass flux is weak due to the weak dust concentration. It occurs only at low levels in COSMO-ART, but is lifted upwards in RegCM. The dust transport is strongly related to the transport of the cold surge and thus, confined to the lower levels. The dust distribution and concentrations are modified due to orographical effects.

3.2 *PRE–SUMMER MONSOON DUST EVENT IN JUNE*

The synoptic conditions and the dust distribution for the period between 9-14 June 2006 are described in detail by Flamant et al. (2009). Strong Harmattan winds were observed over Niger, Chad and Sudan during the first 2 to 4 days of this event, resulting in large uplift of mineral dust. A high pressure system centred on the coasts of Tunisia and Libya dominated North Africa. The southern part of West Africa was characterised by weak sea level pressure gradients. This lead to numerous dust sources during this period with the two main source areas Chad and nearby Niger (9-12 June) related to the Bodélé depression area, and regions of northern Sudan (9-10 June). Large aerosol loads were observed over Niger on 9 June. The aerosols are advected westward between 9-14 June. On 11 June a MCS was initiated at the border Togo and Burkina Faso (not shown), grew into a mature MCS and moved across West Africa. In the afternoon hours on 13 June 2006, a second large MCS developed in the vicinity of the Jos plateau (Nigeria) and travelled across Benin in the morning of 14 June. At the leading edge of the cold pool dust was uplifted but only at small concentrations, as at this time of the year the surface was mostly vegetated. The downdraughts and the stratiform region of the MCS mostly washed out dust in the PBL. Flamant et al. (2009) observed that the dust distribution was affected by the widespread subsidence in the wake of the MCS. They did not observe wet scavenging because the AEJ transported new dust rich air into this region.

The dust emission in the Bodélé depression, Chad and northern Sudan depends on the strength of the northeasterly Harmattan winds associated with the large scale circulation. Dust is transported from the eastern Saharan sources southwest towards the Sahel and the Gulf of Guinea (Flamant et al., 2009). At the ITD the dust layer rises over the southwesterly monsoon flow and into the AEJ. The jet is responsible for the westwards transport. The diurnal variability in the dust source emission can be seen in the dust load advected by the AEJ (Flamant et al., 2009).

On 8 June 2006 at 16 UTC, a dust event is initiated due to the gust front of a convective system over south Algeria (at around 20 °N, 5 °E). This dust event is visible in the SEVIRI satellite images from 19 UTC on (Fig. 4a,b). This case was simulated with COSMO-ART with a horizontal resolution of 28 km. The gust front is only weakly represented in the model (e.g. Fig. 4d at about 5 °W-3 °E, 27-32 °N) due to the coarse resolution. However, a wind maximum due to orographical effects can be observed in the COSMO run. Relatively moist air is transported northwards on the eastern fringes of the Saharan heat low. The Hoggar Mountains in southern Algeria lead to a canalisation of the wind, giving an elongated band of high AOT in the model results (Fig. 4e,f). The dust is transported north–northwestward and the Saharan heat low moves toward Morocco. The dust appears to remain almost stationary to the east of the Atlas Mountains. On 11 June at about 12 UTC (not shown), a low pressure system develops in the lee of the Atlas Mountains which moves towards the east. This system transports a large amount of dust towards north-northeast. The remaining dust is transported by an AEW over West Africa and over the Atlantic.

A second large dust event is initiated in Chad on 9 June 2006 at about 10 UTC (Fig. 4c,d). The COSMO-ART run, initiated on 8 June 2006, 12 UTC, represents this dust event nicely (Fig. 4), although the region where the dust is emitted occurs about 2 ° too far north. Another dust event is initiated about 24 hours later (Fig. 4i,j). Significant amounts of dust are transported northwestwards (towards southern Algeria and northern Niger). The southern part of this dust event is transported westwards and reaches the coast of Mauritania on 12 June.

The period between 13 June, 00 UTC and 14 June, 00 UTC was simulated by two models: the regional climate model RegCM that was initialised on 15 May 2006 and has a horizontal resolution of 60 km, and Meso-NH with a horizontal resolution of 20 km initialised on 7 July 2006 at 00 UTC. Similar dust events are identified, but the position and intensity of dust events in the Saharan and Sahel region differ.

The mass flux of the dust concentration along the selected cross sections shows differences in the dust load (Fig. 5) as would be expected given the different model wind fields and AOTs. The zonal wind field and the dust distribution have certain similar features. Both models show that large amounts of dust are uplifted between about 18-22 °N. The position and strength of the AEJ (Fig. 5) is rather similar over land but the extension over the Atlantic is very different in N–S extent and loca-

tion. This leads to significant differences in the mass flux at 20 °W. The westerly flow to north is similar at upper–levels but the extension to the surface and the south differs. Easterly flow extends further north at 20 °W in Meso-NH. The mass flux in the AEJ is generally stronger in Meso-NH. The strongest mass flux in AEJ occurs at 10 °W in Meso-NH.

3.3 *SUMMER MONSOON DUST EVENT IN JULY*

Dust emissions over the Sahel associated with strong near–surface winds in the region of the West African ITD occurred between July 2006, when the ITD was located over Niger and Mali at around 18 °N (Bou Karam et al., 2008). The dust event occurring between 2 to 12 July 2006 was simulated with the numerical model Meso-NH (Bou Karam et al., 2009b). It has a horizontal resolution of 20 km and was initialised on 2 July 2006 at 00 UTC. The model set up is described in detail in Bou Karam et al. (2009a). They compared the model results with airborne Lidar observations, the SEVIRI Satellite images and AERONET stations in Niamey and Banizoumbou. They showed that model is able to simulate the the dust mobilisation due to strong near–surface winds and the dust aerosol field at the ITD in general.

Several dust events occurred during the modelled period. The events on 5-7 July are described in detail by Bou Karam et al. (2008, 2009a). North of the ITD, the northeasterly flow is modulated by the presence of orography and strong winds occur in association with the formation of nocturnal low–level jets. South of the ITD the southwesterly monsoon flow can be found. Between 2-12 July the ITD moved northwards from 15 °N to 19 °N where it reached the base of the Aïr Mountains ((Bou Karam et al., 2009b)). The large dust uplift was caused by the strong low–level jets north of the ITD in the morning hours just after sunrise. South of the ITD, the emission of mineral dust occurs during the night and in the early morning hours before sunrise. Highly turbulent winds along the leading edge of the monsoon flow lead to dust uplift over the Saharan Sahel (Bou Karam et al., 2008). The circulation in the head of the monsoon density current lifts the mobilised dust towards the wake along an isentropic surface. The stable stratification north of the ITD prevented the dust from reaching altitudes at which it cloud be transported over long distances by the Harmattan. Later in the day turbulent mixing occurred throughout the PBL and the southward transport of the dust by the Harmattan started.

The mass concentration along 10 °E in the RegCM simulation on 5 and 6 July at noon (Fig. 6a,b) are larger than in the Meso-NH cross section (Fig. 6c,d). The maxima occur between 15 and 17 °N on both days in the RegCM run and at around 16 °N on 5 July in the Meso-NH run. The mass concentrations are distinctly lower on 6 July. A second maximum occurs at around 26 °N. Mass concentration can be observed two degrees north and south of it in the RegCM run. In the RegCM run, the dust concentrations are not only higher, but reach also higher altitudes (around 700 hPa), whereas the main concentration are restricted below 900 hPa in the Meso-NH run. Weaker concentrations, however, reach up to 700 hPa. This illustrates nicely, that the dust is transported southwards by the Harmattan.

3.4 *LATE SUMMER MONSOON DUST EVENT IN SEPTEMBER*

On 9 September 2006, a low–level positive vorticity anomaly associated with the westward extension of the Saharan heat low occurred over West Africa at around 5-4 °W, 19-21 °N. It moved along about 18 °N, crossed the West African coast line and then moved towards the southwest, where it merged with a positive vorticity maximum associated with the monsoon depression (Schwendike and Jones, 2010). When this positive vorticity anomaly was collocated with the vorticity maximum of the AEW, out of which Hurricane Helene (2006) developed, the development of the pre–Helene tropical depression was initiated. This secondary heat low circulation led to strong wind speeds near the surface and, thus, to the emission of significant amounts of mineral dust. Dust was also emitted by the gust fronts of the convective systems over land, and due to orographical effects at the Algerian Mountains. The dust was transported over the Atlantic in the SAL. Relatively high values of AOD (not shown) occurred north and northeast of the convective systems that developed into a tropical depression, and were present in the vicinity of the storm during the whole genesis period of Helene.

The dust is uplifted isentropically (not shown) at the ITD (Bou Karam et al., 2008) and reaches the height of the AEJ (600 hPa). The AEJ transports the dust across the Atlantic. The beginning of the dust uplift is distinct in the cross sections over land (Fig. 7). The largest differences between the COMSO-ART run and the RegCM run occur in the cross section over water (Fig. 7a,b) as previously seen in section 3.2. The height of the AEJ is located at about 600 hPa between 14 and 15 °N. In the RegCM simulation it occurs at slightly higher levels and most importantly about 6 ° further north. This results in different mass fluxes. Note, high mass fluxes near the surface are related to the high wind speed values in these regions. Another marked difference between the RegCM and the COSMO-ART run is that the height of the monsoon layer extends up to 450 hPa, whereas in the COMSO-ART run it does not exceed 600 hPa. The position of the AEJ is similar along 15 °W, but differs along 10 °W with the AEJ being located too far north. The cross section along 20 °W based on the COSMO-ART run (Fig. 7f) illustrates that the dust laden air is uplifted and the maximum mass flux occurs just below the jet maximum. Compared to the cross section along 20 °W of the previous case studies, the highest mass flux is observed here.

4. SUMMARY AND CONCLUSION

During 2006 several intense dust events occurred in West Africa. The largest dust load occurred in in late spring and

early summer in accordance to the observations by Engelstaedter and Washington (2007). The first major dust event in 2006 occurred in March in relation to a cold front that first crossed the Atlas Mountains and then moved towards southwest, south and southeast. Canalisation effects at the Hoggar , Aïr and Tibetsi Mountains lead to AOTs up to about 3. The cold front transported the dust across West Africa mainly restricting the dust layer to low–levels.

When West Africa enters the monsoon regime, the mechanism for dust uplift changes. The strong northeasterly Harmattan winds lead to dust emission predominantly in the Bodélé depression, in Chad and in northern Sudan. The dust is the often transported towards the Sahel and the Gulf of Guinea (Flamant et al., 2009) or to region where the AEJ can carry it westward. Another important dust source is the ITD. This was observed in the June, July and September period. The jet is responsible for the fast westwards transport. In the July case, the uplifted dust was transported south by the Harmattan winds. In June, a combination of several dust events led to the large dust load over West Africa. A third important dust lifting mechanism responsible for increasing dust loads in June and September, is the gust front of mesoscale convective systems. Depending on the vegetation, considerable amounts of dust are uplifted at the leading edge of the cold pool, especially during the monsoon onset.

These processes result in a large temporal and spatial (horizontal and vertical) variability of the atmospheric dust load over West Africa. The dust is mainly transported by the AEJ at about 600 hPa, the Harmattan winds and frontal systems at lower levels. The diurnal variability in the dust source emission can also be seen in the dust load advected by the AEJ (Flamant et al., 2009).

The model comparison for the different dust events showed that differences occurred due to different model domains and different model initialisation times. This is a crucial point when aiming to compare different models. This is why the dust load in the COSMO-ART runs, especially in the eastern part of the models domain, is always too small. The dust advected from previous events could not be taken into account. On the other hand, the northern boundary of the the RegCM model run appears to be too far south to fully capture the March event. All three models have a relatively coarse horizontal resolution with 60, 28 and 20 km. Convection is parametrised and the dust emission due to the gust front of MCSs is not realistically simulated. In the future it would be helpful to look into the different models with more detail to understand why they differ from each other. The position of the AEJ differed significantly between the models over the ocean, resulting in a different mass fluxes.

We showed the variability of the dust transport across West Africa based on the monthly mean mass fluxes and the individual cases. Difficulties occurred when comparing the model runs with their different model domains, initialisation times and horizontal resolutions. This shows that a careful comparison of the emission and transport of mineral dust in different models for a single event is needed.

Acknowledgement

Based on a French initiative, AMMA was built by an international scientific group and is currently funded by a large number of agencies, especially from France, UK, US and Africa. It has been the beneficiary of a major financial contribution from the European Community's Sixth Framework Research Programme. Detailed information on scientific coordination and funding is available on the AMMA International web site http://www.amma-international.org.

REFERENCES

Alfaro, S. C. and L. Gomes, 2001: Modeling mineral aerosol production by wind erosion: emission intensities and aerosol size distributions in source areas. *J. Geophys. Res.*, **106**, 18 075–18 084.

Bou Karam, D., C. Flamant, P. Knippertz, O. Reitebuch, P. Pelon, M. Chong, and A. Dabas, 2008: Dust emissions over the Sahel associated with the West African Monsoon inter-tropical discontinuity region: a representative case study. *Q. J. R. Meteorol. Soc.*, **134**, 621–634.

Bou Karam, D., C. Flamant, M. C. T. P. Tulet, J. Pelon, and E. Williams, 2009a: Dry cyclogenesis and dust mobilization in the inter tropical discontinuity of the West African monsoon: a case study. *J. Geophys. Res.*, **114**, D05 115, doi:10.1029/2008JD010952.

Bou Karam, D., C. Flamant, P. Tullet, J.-P. Chaboureau, A. Dabas, and M. C. Todd, 2009b: Estimate of Sahelian dust emissions in the intertropical discontinuity region of the West African monsoon. *J. Geophys. Res.*, **114**, D05 115, doi:10.1029/2008JD010952.

Doms, G. and U. Schättler, 2002: A description of the nonhydrostatic regional model LM. Part I: Dynamics and Numerics. COSMO documentation, Deutscher Wetterdienst, Offenbach, Germany, www.cosmo-model.org.

Engelstaedter, S. and R. Washington, 2007: Temporal controls on global dust emissions: the role of surface gustiness. *Geophys. Res. Lett.*, **24**, L15 805, doi:10.1029/2007GL029971.

Flamant, C., J.-P. Chaboureau, D. J. Parker, C. M. Taylor, J.-P. Cammas, O. Bock, F. Timouk, and J. Pelon, 2007: Airborne observations of the impact of a convective system on the planetary bounday layer thermodynamics and aerosol distribution in the West African monsoon inter-tropical discontinuity region. *Q. J. R. Meteorol. Soc.*, **133**, 1–28.

Flamant, C., C. Lavaysse, M. C. Todd, J.-P. Chaboureau, and J. Pelon, 2009: Multi-platform observations of a representative springtime case of Bodélé and Sudan

dust emission, transport and scavenging over West Africa. *Q. J. R. Meteorol. Soc.*, **135**, 413–430.

Giorgi, F., M. Marinucci, G. T. Bates, and G. D. Canio, 1993: Development of a second generation regional climate model (RegCM2) Part II: Convective processes and assimilation of lateral boundary conditions. *Mon. Wea. Rev.*, **121**, 2814–2832.

Grams, C. M., S. C. Jones, J. Marsham, D. J. Parker, J. M. Haywood, and V. Heuveline, 2010: The Atlantic inflow to the Saharan heat low: observations and modelling. *Q. J. R. Meteorol. Soc.*, **136(s1)**, 125–140.

Grini, A., P. Tulet, and L. Gomes, 2006: Dusty weather forecasts using the Meso-NH mesoscale atmospheric model. *J. Geophys. Res.*, **111**, D19205, doi:10.1029/2005JD007007.

Knippertz, P., 2008: Dust emissions in the West African heat trough - the role of the diurnal cycle and of extratropical disturbances. *Meteorol. Z.*, **17**, 001–011.

Knippertz, P., C. Deutscher, K. Kandler, T. Müller, O. Schulz, and L. Schütz, 2007: Dust mobilization due to density currents in the Atlas region: observations from the SAMUM 2006 field campaign. *J. Geophys. Res.*, **111**, D21109, doi:10.1029/2007JD008774.

Knippertz, P. and A. Fink, 2006: Synoptic and dynamic aspects of an extreme springtime Saharan dust outbreak. *Q. J. R. Meteorol. Soc.*, **132**, 1153–1177.

Lafore, J.-P., J. Stein, N. Asencio, P. Bougeault, V. Ducrocq, J. Duron, C. Fischer, P. Héreil, P. Mascart, V. Masson, J. P. Pinty, J. L. Redelsperger, E. Richard, and J. V.-G. de Arellano, 1998: The Meso-NH atmospheric simulation system: Part I. Adiabatic formulation and control simulations. *Ann. Geophys.*, **16**, 90–109.

Marsham, J. H., D. J. Parker, C. M. Grams, C. M. Taylor, and J. M. Haywood, 2008: Uplift of Saharan dust south of the intertropical discontinuity. *J. Geophys. Res.*, **113**, doi:10.1029/2008JD009844.

Pal, J. S., F. Giorgi, X. Bi, N. Elguindi, F. Solmon, X. Gao, S. A. Rauscher, R. Francisco, A. Zakey, J. Winter, M. Ashfaq, F. S. Syed, J. L. Bell, N. S. Diffenbaugh, J. Karmacharya, A. Konaré, D. Martinez, R. P. da Rocha, L. C. Sloan, and A. L. Steiner, 2007: Regional climate modeling for the developing world: the ICTP RegCM3 and RegCNET. *Bull. Amer. Meteor. Soc.*, **88**, 1395–1409.

Schwendike, J., 2010: Convection in an African easterly wave over West Africa an the eastern Atlantic: a model case study of Helene (2006) and its interaction with the Saharan air layer. Ph.D. thesis, Karlsruhe Institut of Meteorology, Karlsruhe, Germany.

Schwendike, J. and S. C. Jones, 2010: Convection in an African Easterly Wave over West Africa an the eastern Atlantic: a model case study of Helene (2006). *Q. J. R. Meteorol. Soc.*, **136(s1)**, 364–396.

Solmon, F., M. Mallet, N. Elguindi, F. Giorgio, A. Zakey, and A. Konaré, 2008: Dust aerosol impact on regional precipitation over western Africa, mechanisms and sensitivity to absorption properties. *Geophys. Res. Lett.*, **35**, L24705.

Stanelle, T., 2008: Wechselwirkungen von Mineralstaubpartikeln mit thermodynamischen und dynamischen Prozessen in der Atmosphäre über Westafrika. Ph.D. thesis, Institut für Meteorologie und Klimaforschung, Universität/Forschungszentrum Karlsruhe, Karlsruhe, Germany.

Stanelle, T., B. Vogel, H. Vogel, D. Bäumer, and C. Kottmeier, 2010: Feedback between dust particles and atmospheric processes over West Africa in March 2006 and June 2007. *Atmos. Chem. Phys. Discuss.*, **10**, 7553–7599.

Todd, M. C., S. Raghavan, G. Lizcano, and P. Knippertz, 2008: Regional model simulations of the Bodélé low-level jet of northern Chad during the Bodélé Dust Experiment (BoDEx 2005). *J. Climate*, **21**, 995–1012.

Tulet, P., V. Crassier, F. Cousin, K. Suhre, and R. Rosset, 2005: ORILAM, a three moment lognormal aerosol scheme for mesoscale atmospheric model. On-line coupling into the Meso-NH-C model and validation on the Escompte campaign. *J. Geophys. Res.*, **110**, doi:10.1029/2004JD009871.

Vogel, B., C. Hoose, H. Vogel, and C. Kottmeier, 2006: A model of dust transport applied to the Dead Sea area. *Meteorol. Z.*, **15**, DOI: 10.1127/0941–2948/2006/0168.

Vogel, B., H. Vogel, D. Bäumer, M. Bangert, K. Lundgren, R. Rinke, and T. Stanelle, 2009: The comprehensive model system COSMO-ART - radiative impact of aerosol on the state of the atmosphere on the regional scale. *Atmos. Chem. Phys.*, **9**, 8661–8680.

Wang, H., G. Shi, S. Li, W. Li, B. Wang, and Y. Huang, 2006: The impacts of optical properties on radiative forcing due to dust aerosol. *Adv. Atmos. Sci.*, **23**, 431–441.

Washington, R. and M. C. Todd, 2006: Atmospheric controls on mineral dust emission from the Bodélé depression, Chad: intraseasonal to interannual variability and the role of the low level jet. *Geophys. Res. Lett.*, **32**, L17701, doi:10.1029/2005GL023597.

Zakey, A. S., F. Solmon, and F. Giorgi, 2006: Development and testing of a desert dust module in a regional climate model. *Atmos. Chem. Phys.*, **6**, 1749–1792.

Zender, C., H. Bian, and D. Newman, 2003: The mineral dust entrainment and deposition model DEAD: description and 1990s dust climatology. *J. Geophys. Res.*, **108**, doi:10.1029/2002JD002775.

Table 1: Details of the model runs used in this study.

Dates	Model	Model Domain	Resolution	Initialisation Time
15 Dec. 2005–31 Dec. 2006	RegCM	34.7 °W-50.2 °E, 5.5 °N-30.5 °N	60 km	15/12/2005, 00 UTC
15 Feb.–31 May 2006	RegCM	34.7 °W-50.2 °E, 5.5 °N-30.5 °N	60 km	15/02/2006, 00 UTC
15 May–31 Sept. 2006	RegCM	34.7 °W-50.2 °E, 5.5 °N-30.5 °N	60 km	15/05/2006, 00 UTC
5–10 March 2006	COSMO-ART	23 °W-20 °E, 0.5-40 °N	28 km	05/03/2006, 00 UTC
7–14 June 2006	Meso-NH	23.5 °W-33.5 °E, 0.4-35.7 °N	20 km	07/06/2006, 00 UTC
8–13 June 2006	COSMO-ART	41 °W-41 °E, 0-35 °N	28 km	08/06/2006, 12 UTC
12–15 June 2006	COSMO-ART	41 °W-41 °E, 0-35 °N	28 km	12/06/2006, 12 UTC
2–10 July 2006	Meso-NH	2 °W-16 °E, 12-29 °N	20 km	02/07/2006, 00 UTC
9–14 Sept. 2006	COSMO-ART	60 °W-12 °E, 1-40 °N	28 km	09/09/2006, 12 UTC

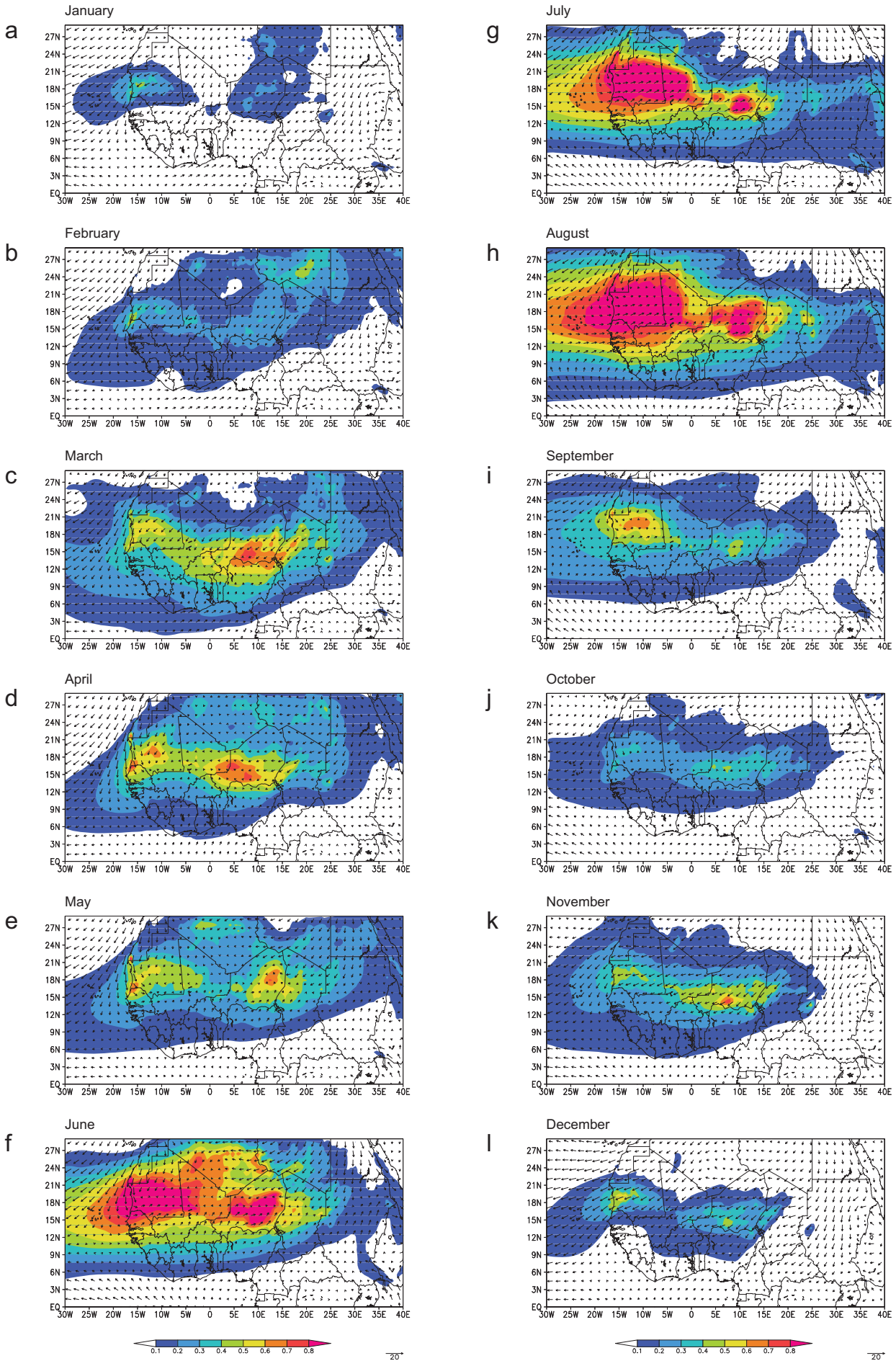

FIG. 1: The monthly mean aerosol optical thickness (AOT) and the mean wind speed at 700 hPa ($m\,s^{-1}$) for the months of 2006 based on RegCM model runs.

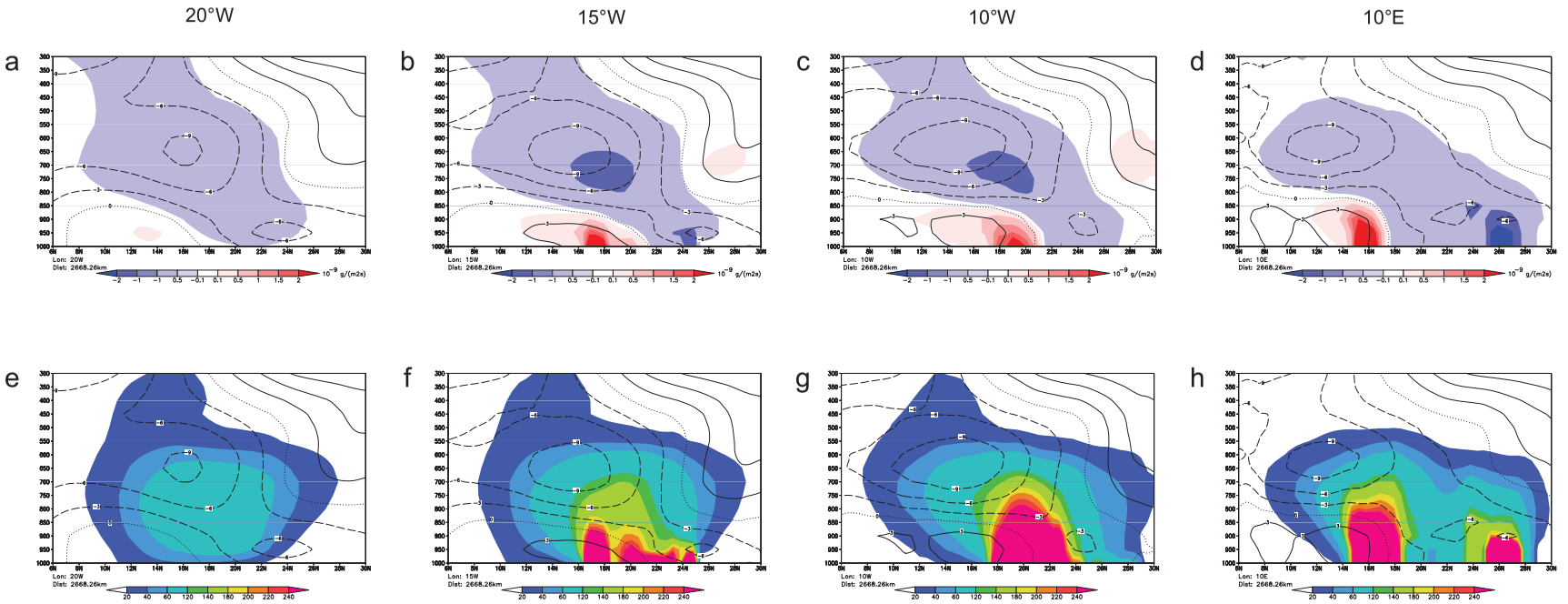

FIG. 2: (a-d) Cross sections along 20 °W, 15 °W, 10 °W, 10 °E display mean mass flux of mineral dust through the section for the period May to September($g\,m^{-2}\,s-1$)based on the model run with RegCM with a horizontal resolution of 60 km. (e-h) The same as for (a-d) but mass concentration. Pressure (hPa) is used as the vertical coordinate.

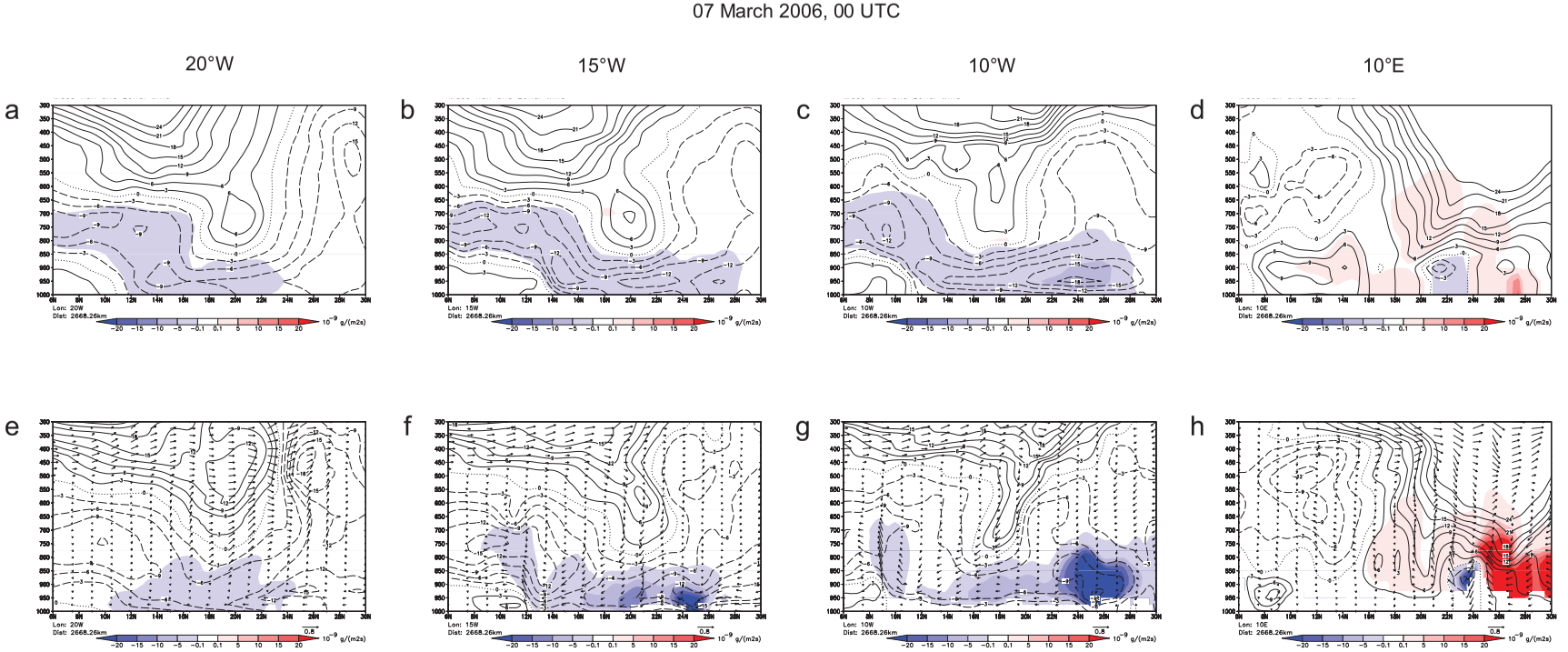

FIG. 3: (a-d) Cross sections ($g\,m^{-2}\,s-1$) along 20 °W, 15 °W, 10 °W, 10 °E display mass flux of mineral dust through the section based on the model run with RegCM, initialised on 1 March 2006, 00 UTC and with a horizontal resolution of 60 km. (e-h) The same as for (a-d) and the zonal wind (contour interval is $3\,m\,s^{-1}$) based on a COSMO-ART run initialised on 5 March 2006, 00 UTC, and a horizontal resolution of 28 km. The displayed time is 7 March 2006 at 00 UTC. Pressure (hPa) is used as the vertical coordinate.

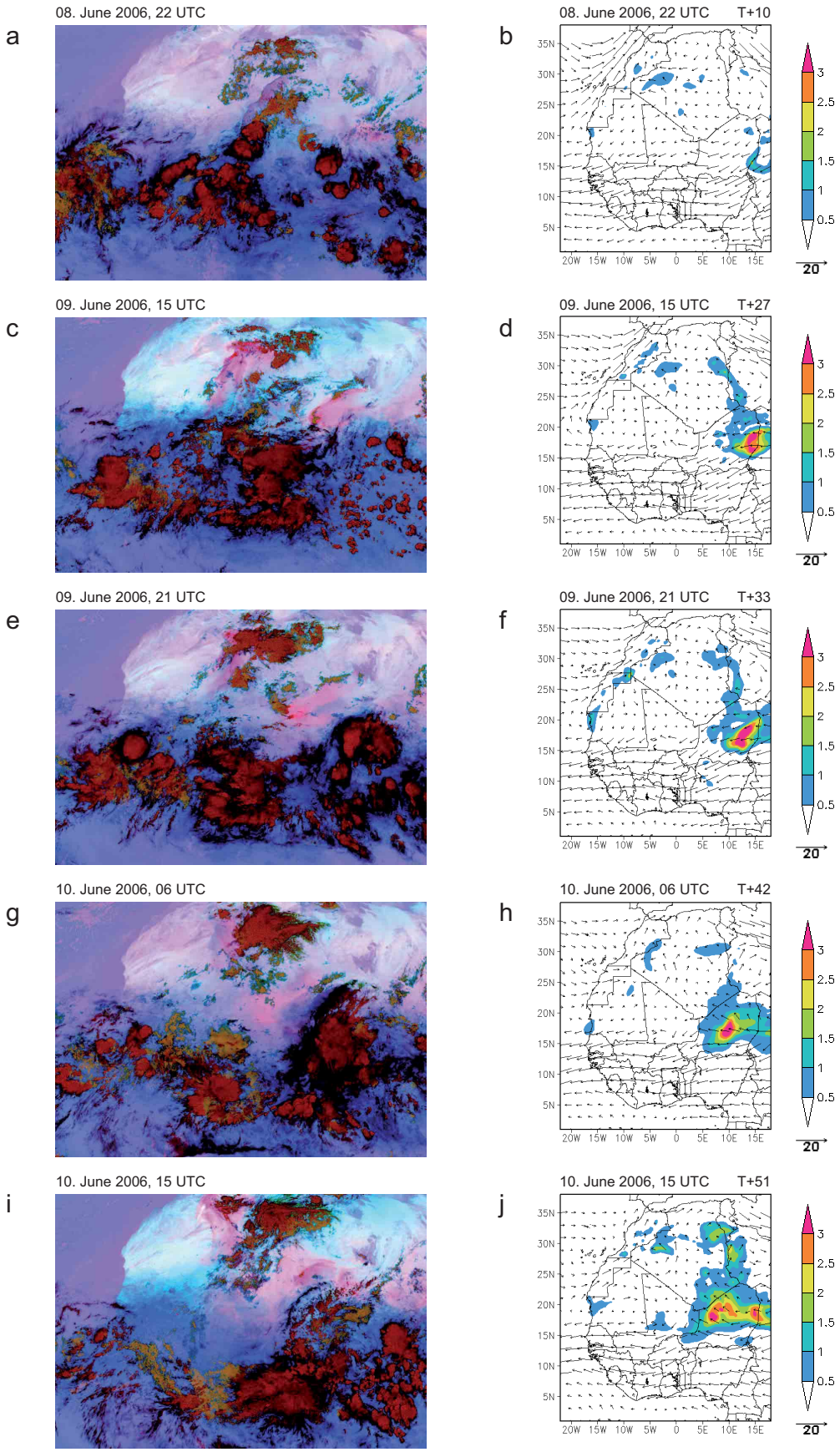

FIG. 4: Left: The SEVIRI false colour images. Dust particles are displayed in pink and the deep cold cloud tops in dark red. The top left corner has the coordinates 25 °W, 32 °N, the top right corner 35 °E, 32 °N, the bottom left corner 25 °W, 0 °, and bottom right corner 35 °E, 0 °. Right: The aerosol optical thickness and the horizontal wind at 700 hPa ($m\,s^{-1}$) based on the COSMO-ART run initialised on 8 June 2006 at 12 UTC.

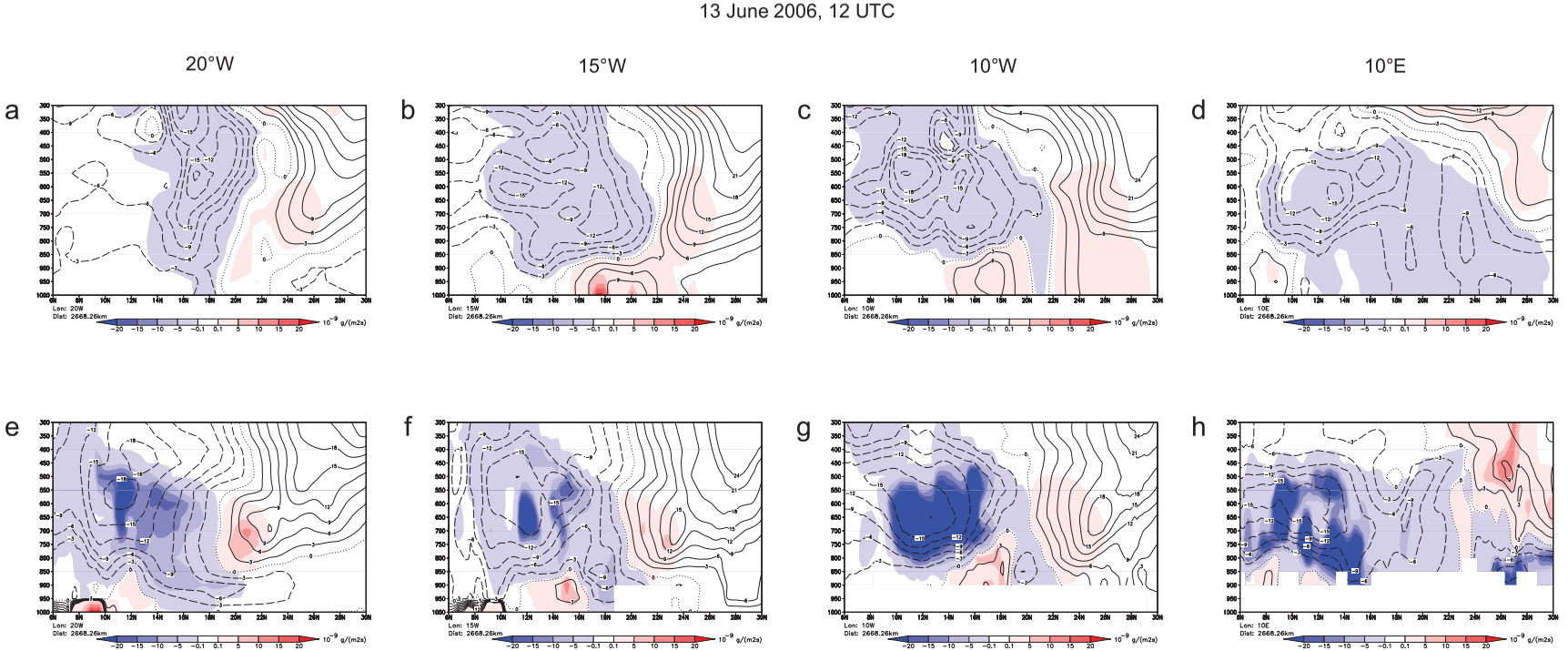

FIG. 5: The same as in Figure 3, but for the RegCM model run initiated on 15 May 2006, 00 UTC (a-d), and the Meso-NH model run initiated on 7 June 2006, 00 UTC (e-h). The displayed time is 13 June 2006 at 12 UTC. Note, no data is available below 900 hPa due to artifacts during the interpolation from model level to pressure levels.

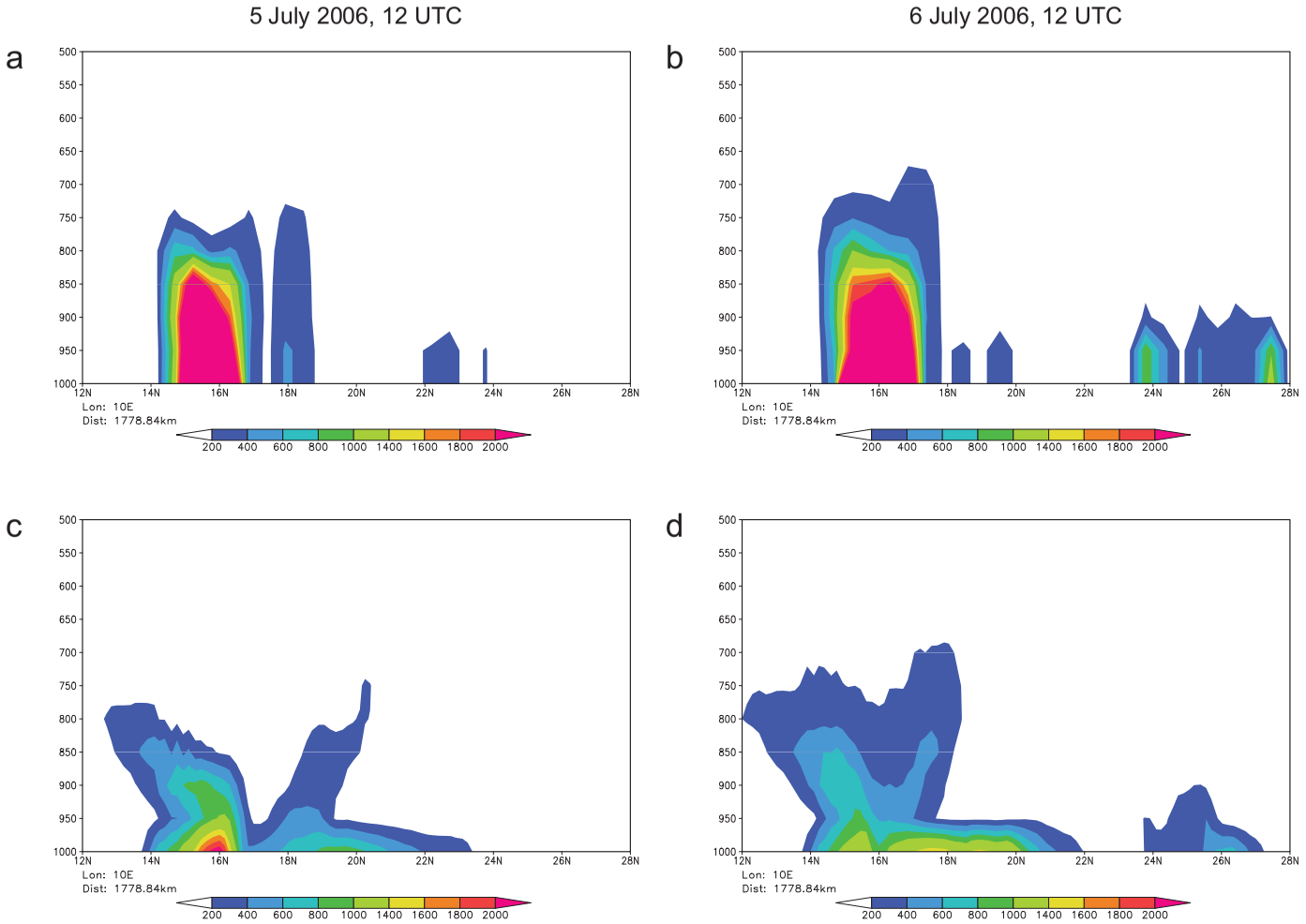

FIG. 6: The same as Figure 3but along 10 °E based on the RegCM run initialised on 15 June 2006, 00 UTC (a-b) and based on the Meso-NH run initialised on 2 July 2006, 00 UTC (c,d).

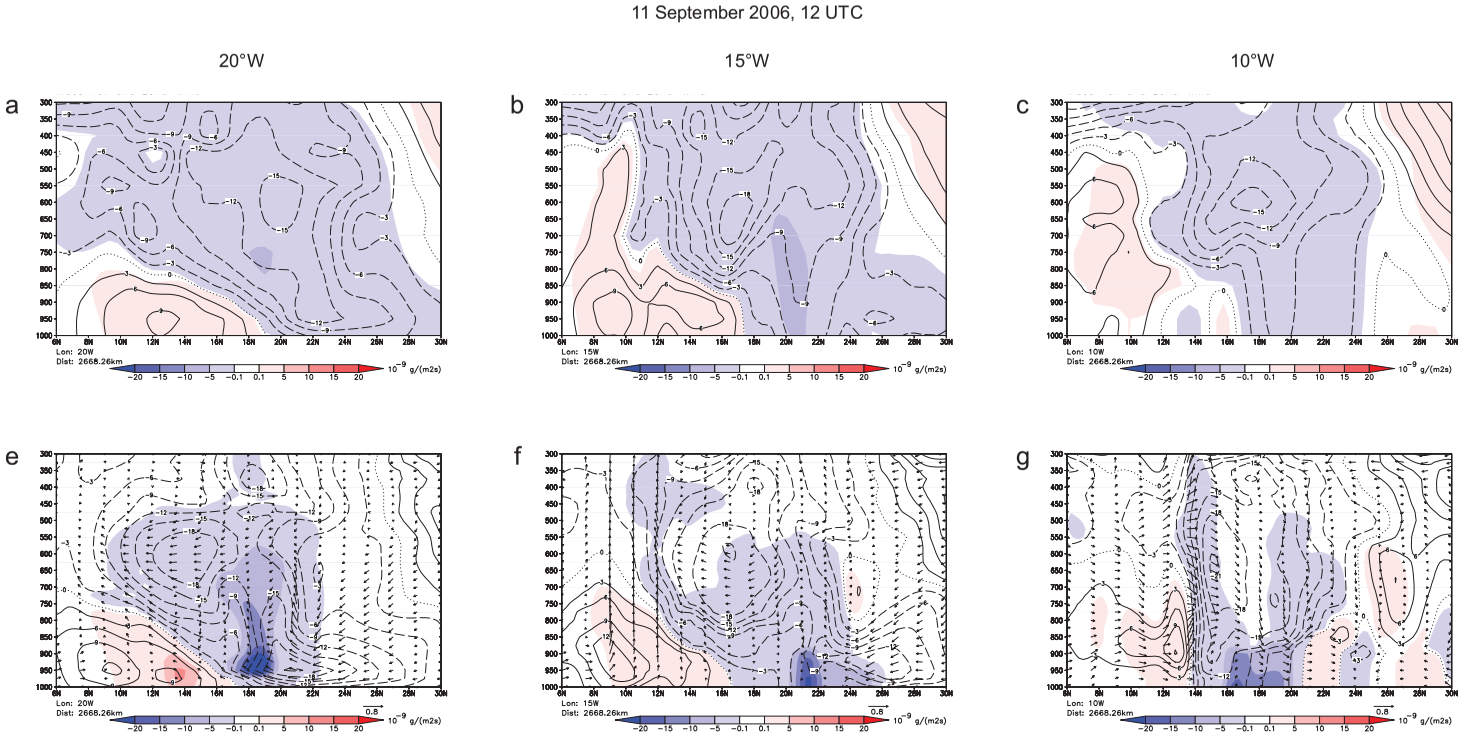

FIG. 7: The same as Figure 3but along 20 °W, 15 °W, 10 °W based on the RegCM run initialised on 15 May 2006, 00 UTC (a-d) and based on the COSMO-ART run initialised on 9 September 2006, 12 UTC.